View metadata, citation and similar papers at core.ac.uk

brought to you by CORE

provided by Open Archive Toulouse Archive Ouverte

Open Archive Toulouse Archive Ouverte (OATAO)

OATAO is an open access repository that collects the work of some Toulouse researchers and makes it freely available over the web where possible.

This is an author's version published in: https://oatao.univ-toulouse.fr/19914

Official URL: http://doi.org/10.1109/WFCS.2018.8402346

To cite this version :

Finzi, Anaïs and Mifdaoui, Ahlem and Frances, Fabrice and Lochin, Emmanuel Incorporating TSN/BLS in AFDX for Mixed-Criticality Applications: Model and Timing Analysis. (2018) In: 14th IEEE International Workshop on Factory Communication Systems, 13 June 2018 - 15 June 2018 (Imperia, Italy).

Any correspondence concerning this service should be sent to the repository administrator:
tech-oatao@listes-diff.inp-toulouse.fr

Incorporating TSN/BLS in AFDX for Mixed-Criticality Applications: Model and Timing Analysis

A. FINZI, A. MIFDAOUI, F. FRANCES, E. LOCHIN
University of Toulouse-ISAE, France

***Abstract*—In this paper, we model and analyse the timing performance of an extended AFDX standard, incorporating the Burst Limiting Shaper (BLS) proposed by the Time Sensitive Networking group. The extended AFDX will enable the interconnection of different avionics domains with mixed-criticality levels, e.g., current AFDX traffic, Flight Control and In-Flight Entertainment. First, we present the model and the worst-case timing analysis, using the Network Calculus framework, of such an extended AFDX to infer real-time guarantees. Secondly, we conduct its performance evaluation on a representative AFDX configuration. Results show the tightness of the proposed model, with reference to simulation results. Moreover, they confirm the efficiency of incorporating the BLS in the AFDX standard to noticeably enhance the medium priority level delay bounds, while respecting the higher priority level constraints, in comparison with the current AFDX standard.**

I. INTRODUCTION

The growing number of interconnected end-systems and the expansion of exchanged data in avionics have led to an increase in complexity of the communication architecture. To cope with this trend, a first communication solution based on a high rate backbone network, i.e., the AFDX (Avionics Full Duplex Switched Ethernet) [1], has been implemented by Airbus in the A380 to interconnect critical subsystems. Moreover, some low rate data buses, e.g., CAN [11] or ARINC 429[5], are still used to handle some specific avionics domains, such as the I/O process and the Flight Control Management. Although this architecture reduces the time to market, it conjointly leads to inherent heterogeneity and new challenges to guarantee the real-time requirements.

To cope with these emerging issues, with the maturity and reliability progress of the AFDX after a decade of successful use, a homogeneous avionic communication architecture based on such a technology to interconnect different avionics domains may bring significant advantages, such as easier installation and maintenance and reduced weight and costs. This homogeneous communication architecture, based on the AFDX technology, needs to support mixed-criticality applications, where safety-critical and best effort traffic coexist. Hence, in addition to the current AFDX traffic profile, called Rate Constrained (RC) traffic, at least two extra profiles have to be handled. The first, denoted by Safety-Critical Traffic (SCT), is specified to support flows with hard real-time constraints and the highest criticality, e.g., flight control data; whereas the second is for Best-Effort (BE) flows with no delivery constraint and the lowest criticality, e.g., In-Flight Entertainment traffic.

As a first step, we have studied in [4] different existing solutions to enable mixed-criticality applications in the AFDX standard. Then, we have selected the most promising one: the Burst Limiting Shaper (BLS) proposed by the IEEE 802.1Q Time Sensitive Networking task group, to be incorporated in the AFDX due to its fairness and low complexity. We have also showed the improved schedulability level and delay bounds of such a proposal through simulations. However, it is well-known that it is difficult to draw firm conclusions concerning the solution performance based on simulations, since it does not cover the worst-case behaviour. The latter is a key point to prove certification requirements and needs formal analysis.

Therefore, our main contributions in this paper are twofold: (i) first in Section III, the formal timing analysis of the extended AFDX (incorporating he TSN/BLS) is conducted using Network Calculus; (ii) second, in Section IV, the performance evaluation of the extended AFDX when varying the maximum utilisation rate of SCT and RC traffics is detailed. The aim is to assess the tightness of the model, in reference to simulation results in [4]; and prove the extended AFDX efficiency to guarantee SCT traffic constraints, while enhancing the RC delays and SCT utilisation rate.

II. BACKGROUND AND RELATED WORK

In this section, we present the BLS mechanism and the main concept of the Network Calculus framework. Then, we review the main worst-case timing analyses of the TSN/BLS shaper.

A. *Burst Limiting Shaper*

The BLS belongs to the credit-based shapers class and it is generally used on top of Non-Preemptive Static Priority (NP-SP) scheduler as shown in Fig.1. It has been defined in [6] by an upper threshold L_M, a lower threshold L_R, such as $0 \leqslant L_R < L_M$, and a reserved bandwidth BW. Additionally, the priority of a queue q shaped by BLS, denoted $p(q)$, can vary between a high and a low value (with 0 the highest), denoted p_H and p_L. The low value is usually below the lowest priority of the unshaped traffic. In the avionic context, to guarantee the safety isolation level between the different traffic profiles, the low value associated to the SCT is set to be lower than the

RC priority level, but higher than the BE priority. Therefore as shown in Fig.1, when considering one class for each traffic type, SCT queue priority oscillates between 0 (the highest) and 2, RC priority is 1 and BE has the priority 3 (the lowest). Thus, when SCT traffic is enqueued, BE traffic can never be sent no matter the state of BLS. In this case, RC is the only traffic that can be sent and this only happens when the SCT priority is 2. As a consequence, BE traffic is isolated from SCT and RC traffics.

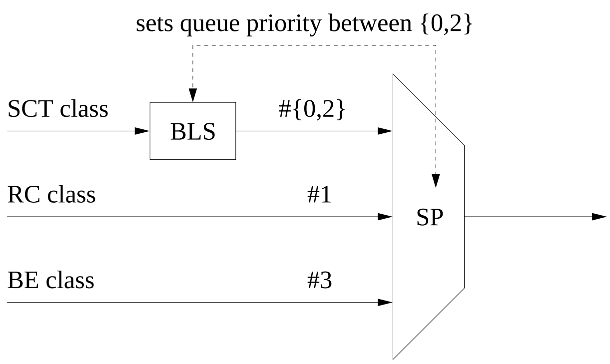

Fig. 1. An extended AFDX switch output port multipelxer architecture

The credit counter varies as follows:
(i) initially, the credit counter starts at 0 and the queue of the burst limited flows is high;
(ii) the main feature of the BLS is the change of priority $p(k)$ of the shaped queue, which occurs in two contexts: 1) if $p(k)$ is high and credit reaches L_M; 2) if $p(k)$ is low and credit reaches L_R;
(iii) when a frame is transmitted, the credit increases (is consumed) with a rate of I_{send}, else the credit decreases (is gained) with a rate of I_{idle};
(iv) when the credit reaches L_M, it stays at this level until the end of the transmission of the current frame (if any);
(v) when the credit reaches 0 it stays at this level until the end of the transmission of the current frame (if any). The credit remains at 0 until a new BLS frame is transmitted.

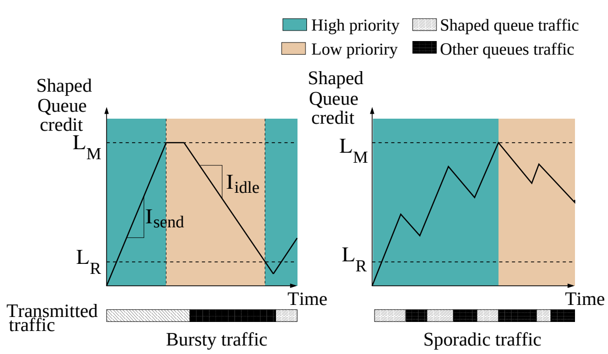

Fig. 2. BLS credit evolution

The behaviour of the BLS is illustrated in Fig. 2. As shown, the credit is always between 0 and L_M. The different parameters of the BLS shaper are defined as follows: (i) the decreasing rate is: $I_{idle} = BW \cdot C$, where C is the link speed and BW is the percentage of bandwidth reserved for BLS frames; (ii) the increasing rate is: $I_{send} = C - I_{idle}$.

It is worth noting that with the BLS, both the priority of the shaped queue and the state of all the queues, i.e., empty or not, define whether the credit is gained or lost. This aspect is depicted in Fig.2 for two arrival scenarios. The first one (left figure) shows the case of a bursty traffic, where the maximum of traffic shaped by the BLS is sent when its priority is the highest. Consequently, the other priorities send as much traffic as possible when the BLS queue priority has the low value. The second one (right figure) is for sporadic traffic, where we can see that when the shaped queue priority is highest but no frame is available, then the credit is regained. However, when the priority is at the low value and the other queues are empty, then shaped queue frames can be transmitted and the credit is consumed.

B. Network Calculus Framework

The timing analysis detailed in this paper is based on Network Calculus theory [8] providing upper bounds on delays and backlogs. Delay bounds depend on the traffic arrival described by the so called *arrival curve* α, and on the availability of the traversed node described by the so called minimum *service curve* β. The definitions of these curves are explained as following.

Definition 1 (Arrival Curve). *[8] A function $\alpha(t)$ is an arrival curve for a data flow with an input cumulative function $R(t)$,i.e., the number of bits received until time t, iff:*

$$\forall t, R(t) \leq R \otimes {}^{1}\alpha(t)$$

Definition 2 (Strict minimum service curve). *[8] The function β is the minimum* strict *service curve for a data flow with an output cumulative function R^*, if for any backlogged period* $]s,t]^2$, $\Delta R^*(t-s) \geq \beta(t-s)$.

Definition 3 (Maximum service curve). *[8] The function $\gamma(t)$ is the maximum service curve for a data flow with an input cumulative function $R(t)$ and output cumulative function $R^*(t)$ iff:*

$$\forall t, R^*(t) \leq R \otimes \gamma(t)$$

The traffic contracts are generally enforced using a leaky-bucket shaper, i.e., the traffic flow is (r,b)-constrained where r and b are the maximum rate and burst, respectively, and the arrival curve is $\alpha(t) = r \cdot t + b$ for $t > 0$. A common model of service curve is the rate-latency curve $\beta_{R,T}$, defined as $\beta_{R,T}(t) = [R(t-T)]^+$, where R for the transmission capacity, T for the system latency, and $[x]^+$ for the maximum between x and 0.

Then, we need the following results to compute the main performance metrics.

[1] $f \otimes g(t) = \inf_{0 \leq s \leq t}\{f(t-s) + g(s)\}$
[2] $]s,t]$ is called backlogged period if $R(\tau) - R^*(\tau) > 0, \forall \tau \in]s,t]$

Theorem 1 (Performance Bounds). *[8] Consider a flow F constrained by an arrival curve α crossing a system $\mathcal{S}$ that offers a minimum service curve β and a maximum service curve γ. The performance bounds obtained at any time t are:*
Backlog[3] *:* $\forall\ t:\ q(t) \leq v(\alpha, \beta)$
Delay[4]*:* $\forall\ t:\ d(t) \leq h(\alpha, \beta)$
Output arrival curve[5]*:* $\alpha^*(t) = (\alpha \oslash \beta)(t)$
Tight Output arrival curve: $\alpha^*(t) = ((\gamma \otimes \alpha) \oslash \beta)(t)$

Theorem 2 (Concatenation-Pay Bursts Only Once). *[8] Assume a flow crossing two servers with respective service curves β_1 and β_2. The system composed of the concatenation of the two servers offers a service curve $\beta_1 \otimes \beta_2$.*

Corollary 1. *(Left-over service curve - NP-SP Multiplexing)[2] Consider a system with the strict service curve β and m flows crossing it, $f_1, f_2, .., f_m$. The maximum packet length of f_i is $l_{i,max}$ and f_i is α_i-constrained. The flows are scheduled by the NP-SP policy, where priority of f_i > priority of $f_j \Leftrightarrow i < j$. For each $i \in \{2, .., m\}$, the strict service curve of f_i is given by*[6]*:*

$$(\beta - \sum_{j<i} \alpha_j - \max_{k \geq i} l_{k,max})_{\uparrow}$$

C. Worst-case Timing Analysis of TSN/BLS Shaper

There are some interesting approaches in the literature concerning the worst-case timing analysis of TSN network, and more particularly BLS shaper. The first and seminal one in [12] introduces a first service curve model to induce worst-case delay computation. However, this presentation published by the TSN task group has never been extended in a formal paper. The second one has detailed a more formal worst-case timing analysis in [13]. However, this approach has some limitations. Basically, the proposed model does not take into account the impact of either the same priority flows or the higher ones, which will clearly induce optimistic worst-case delays. The last and more recent one in [15] has proposed a formal analysis of TSN/BLS shaper, based on a Compositional Performance Analysis (CPA) method. This approach has handled the main limitations of the model presented in [13]; and interesting results for an automotive case study have been detailed. The impact of BLS on the highest priority traffic has been showed to deteriorate its timing performance, in comparison with a classic NP-SP scheduler.

However, in this paper, our main objective is different from [15] and consists in incorporating BLS in the AFDX, denoted as extended AFDX, to guarantee the highest priority traffic deadline, while limiting its impact on the medium one, i.e., RC. Moreover, our worst-case timing analysis is based on the Network Calculus framework, which has been proved as highly modular and scalable, in comparison with CPA [14], and very effective to prove the certification requirements of avionics applications [7]. Several existing works have used Network Calculus to analyse the timing performance of Switched Ethernet and AFDX [7] [10] [9] [3]. However, to the best of our knowledge, the issue of modeling and analysing the TSN/BLS on top of a NP-SP scheduler (as shown in Fig.1), using the Network Calculus has not been handled yet in the literature.

[3]v: maximal vertical distance
[4]h: maximal horizontal distance
[5]$f \oslash g(t) = \sup_{s \geq 0}\{f(t+s) - g(s)\}$
[6]$g_{\uparrow}(t) = \max\{0, \sup_{0 \leq s \leq t} g(s)\}$

III. Timing analysis using NC

In this section, to conduct the worst-case timing analysis of the proposed extended AFDX, we present first our assumptions and the considered metric. Then, to compute the delay bounds, we need to define the service curve of the switch output port multiplexer mux. The latter consists of two types of nodes: a BLS node bls and a NP-SP node sp, as illustrated in Fig.1. Since the NP-SP node has a well-known model (presented in Cor.1), we will focus herein on the model of the BLS node bls. The main notations used in this paper are presented in Table I.

SCT	Safety Critical Traffic
RC	Rate Constrained traffic
BE	Best Effort traffic
C	Link speed
MFS_f	Maximum Frame Size of flow f
BAG_f	Bandwidth Allocation Gap of flow f
L_M, L_R	BLS maximum and resume credit levels
BW	BLS reserved bandwidth
I_{idle}, I_{send}	BLS idle and sending slopes
p_H, p_L	SCT high (H) and low (L) priority levels
UR_k	Utilisation rate of a class k
$\alpha_k^n(t), \alpha_k^{*,n}(t)$	Input and output arrival curve of class k at node n
$\beta_k^n(t)$	Strict minimum service curve offered to class k by node n
$\gamma_k^n(t)$	Maximum service curve offered to class k by node n

TABLE I
Notations

A. Preliminaries and assumptions

First, we model the switch output port, presented in Fig.1, for three traffic classes: i) SCT with a priority switching between $p_H = 0$ and $p_L = 2$; ii) RC with the priority 1; iii) and BE with the priority 3. Consequently, even when the SCT priority is low, the BE has the lowest priority. So, the impact of the BE will be taken into account in the model of the sp node, as shown in Cor.1.

To assess the performance of the BLS, we use the delay bounds of SCT and RC as a metric, since they both have deadlines contrary to BE. To compute the delays bounds within each node $n \in \{bls, sp, mux\}$, we use Th.1 under the following assumptions:

(i) leaky-bucket arrival curves for the traffic flows at the input of node n. For a flow f, we define the Maximum Frame Size MFS_f and the Bandwidth Allocation Gap BAG_f (the period and generally also the deadline). For each class k, the aggregate traffic has an input arrival curve at node n: $\alpha_k^n(t) = r_k^n \cdot t + b_k^n$, where the initial arrival curve sent by the traffic source is $\alpha_k(t) = \sum_{f \in k} \frac{MFS_f}{BAG_f} \cdot t + MFS_f$;

(ii) the offered service curve by node n to the traffic class k is a rate-latency curve: $\beta_k^n(t) = R_k^n \cdot (t - T_k^n)^+$;

(iii) we are concerned herein with the delay bound within one extended AFDX switch. It is worth noting that extending our work to multi-hops may be easily done through considering the sum of delay bounds within each hop, while propagating the arrival curves from one hop to another using Th.1 or through Pay Bursts Only Once principle [8].

Therefore, in each node n and $\forall k \in \{SCT, RC, BE\}$ with $r_k^n \leqslant R_k^n$, based on Th. 1, the delay bound is the maximum horizontal distance between the arrival and service curves: $h(\alpha_k^n, \beta_k^n) = \frac{b_k^n}{R_k^n} + T_k^n$.

B. BLS node model

We detail here the computation of BLS service curves offered to SCT.

The strict minimum and maximum service curves offered to SCT by a bls node are defined in Th.3 and Th.4, respectively.

Theorem 3 (Strict Minimum Service Curve offered to SCT by a BLS node)**.** *Consider SCT traffic crossing the output port with a constant rate C, defined in Fig.1.*

The strict minimum service curve guaranteed to SCT traffic by a bls node is as follows:

$$\beta_{SCT}^{bls}(t) = \left(C - \frac{MFS_{RC}^{sat}}{\Delta_{inter}^{\beta}}\right) \cdot \frac{I_{idle}}{C} \cdot \left(t - \Delta_{idle}^{\beta}\right)^+$$

where:

$$\begin{aligned}
MFS_{RC}^{sat} &= \max(\max_{f \in RC} MFS_f - \frac{C}{I_{idle}} \cdot L_R, 0) \\
\Delta_{inter}^{\beta} &= \min(\frac{\max_{f \in RC} MFS_f}{C} . \frac{I_{idle}}{I_{send}}, \frac{L_R}{I_{send}}) \\
&+ \frac{L_M - L_R}{I_{send}} + \frac{L_M - L_R}{I_{idle}} + \frac{\max_{f \in RC} MFS_f}{C} \\
\Delta_{idle}^{\beta} &= \frac{L_M - L_R}{I_{idle}} + \frac{\max_{f \in RC} MFS_f}{C}
\end{aligned}$$

Proof. The full proof is detailed in the Appendix B. We present here a sketch of proof. The main idea is to compute the consumed and the gained credits. Knowing that the credit is continuous and always between 0 and L_M, we use the sum of the credit variations to compute the minimum service curves of the BLS node bls. The main difficulty consists in computing the traffic sent during saturation times, i.e., when the credit is neither gained nor consumed due to the minimum and maximum levels, 0 and L_M, respectively. □

Theorem 4 (Maximum Service Curve offered to SCT by a BLS node)**.** *Consider SCT traffic crossing the output port with a constant rate C, defined in Fig.1. The maximum service curve guaranteed to SCT is: $\gamma_{SCT}^{bls}(t) = C \cdot t$ in the absence of backlogged RC traffic; otherwise, during a backlogged RC period:*

$$\gamma_{SCT}^{bls}(t) = \frac{\Delta_{send}^{\gamma}}{\Delta_{inter}^{\gamma}} \cdot C \cdot t + b_{SCT}^{max} \cdot \frac{\Delta_{idle}^{\gamma}}{\Delta_{inter}^{\gamma}}$$

where:

$$\begin{aligned}
b_{SCT}^{max} &= \frac{C}{I_{send}} \cdot L_M + \max_{f \in SCT} MFS_f \\
\Delta_{send}^{\gamma} &= \frac{\max_{f \in SCT} MFS_f}{C} + \frac{L_M - L_R}{I_{send}} \\
\Delta_{idle}^{\gamma} &= \frac{L_M - L_R}{I_{idle}} \\
\Delta_{inter}^{\gamma} &= \Delta_{send}^{\gamma} + \Delta_{idle}^{\gamma}
\end{aligned}$$

Proof. The full proof is detailed in the Appendix C. It is based on the same principle as Th.3, i.e., the computation the consumed and the gained credits, to obtain the maximum service curve of node bls. □

Finally, to compute the minimum service curve offered to RC by the output port multiplexer mux, we need the maximum output arrival curve of SCT at the output of the BLS node bls. Based on the defined minimum and maximum service curves in Th.3 and Th.4, respectively, the needed arrival curve is detailed in the following Corollary:

Corollary 2 (Maximum Output Arrival Curve of SCT from BLS node)**.** *Consider a SCT with a leaky-bucket arrival curve α at the input of a BLS node, guaranteeing a minimum service curve β_{SCT}^{bls} (defined in Th.3) and a maximum service curve γ_{SCT}^{bls} (defined in Th.4). The maximum output arrival curve is:*

$$\alpha_{SCT}^{*,bls}(t) = \min(\gamma_{SCT}^{bls}(t), \alpha \oslash \beta_{SCT}^{bls}(t)) \quad (1)$$

Proof. To prove Corollary 2, we generalize herein the rule 13 in p. 123 in [8], i.e., $(f \otimes g) \oslash g \leq f \otimes (g \oslash g)$, to the case of three functions f, g and h when $g \oslash h \in \mathcal{F}$, where $\mathcal{F}$ is the set of non negative and wide sense increasing functions:

$$\mathcal{F} = \{f : \mathbb{R}^+ \to \mathbb{R}^+ \mid f(0) = 0, \forall t \geq s : f(t) \geq f(s)\}$$

According to Theorem 1, we have $\alpha^*(t) = (\gamma_{SCT}^{bls} \otimes \alpha) \oslash \beta_{SCT}^{bls}$. Moreover, in the particular case of a leaky-bucket arrival curve α and a rate-latency service curve β_{SCT}^{bls}, $\alpha \oslash \beta_{SCT}^{bls}$ is a leaky-bucket curve, which is in $\mathcal{F}$. Hence, we have the necessary condition to prove the following:

$$(\alpha \otimes \gamma) \oslash \beta(t) \leq \gamma \otimes (\alpha \oslash \beta)(t) \leq \min(\gamma(t), \alpha \oslash \beta(t))$$

□

Now that the BLS node has been modelled, we detail the computation of the minimum service curves offered to SCT and RC by the output port multiplexer mux.

C. Switch output port multiplexer modelisation

We start with the strict minimum service curve offered to SCT, detailed in the following Theorem:

Theorem 5 (Strict Minimum Service Curve offered to SCT by an output port multiplexer)**.** *Consider the output port defined in Fig.1 with a constant rate C, and serving the traffic classes f_k with $k \in \{SCT, RC, BE\}$. Consider α_k-constrained traffic class k, the strict minimum service curve offered to SCT by the output port multiplexer is:*

$$\beta_{SCT}^{mux}(t) = \max\left(\beta_{SCT,p_L}^{sp}, \beta_{SCT}^{bls} \otimes \beta_{SCT,p_H}^{sp}\right)(t)$$

with:

- $\beta^{sp}_{SCT,p_L}(t) = (C\cdot t - \alpha_{RC}(t) - \max_{f\in BE\cup SCT} MFS_f)_\uparrow$ *the strict minimum service curve offered by the NP-SP node sp when the SCT priority is low;*

- $\beta^{bls}_{SCT}(t)$ *the strict minimum service curve offered by the BLS node bls to SCT, defined in Th.3;*

- $\beta^{sp}_{SCT,p_H}(t) = (C\cdot t - \max_{f\in All} MFS_f)_\uparrow$ *the strict minimum service curve offered by the NP-SP node sp when the SCT priority is high and $All = \{SCT \cup RC \cup BE\}$.*

Proof. The idea is to model the impact of a BLS implemented on top of the NP-SP scheduler on SCT. To achieve this aim, we distinguish two possible scenarios. The first one covers the particular case where the SCT priority remained low, i.e., the other queues are empty; whereas the second one covers the general case where the priority of SCT oscillates between p_L and p_H, as explained in Section II-A. Firstly, the minimum service curve guaranteed within mux in the first scenario is due to the NP-SP scheduler and denoted β^{sp}_{SCT,p_L}, which is computed via Corollary 1 when considering the impact of traffics with a priority higher or equal than p_L (RC traffic). Secondly, the minimum service curve guaranteed within mux in the second scenario is computed via Th.2, through the concatenation of the service curves within the BLS node β^{bls}_{SCT} (computed in Th.3) and the NP-SP node β^{sp}_{SCT,p_H} (computed via Corollary 1 when SCT has the highest priority). □

Theorem 6 (Strict Minimum Service Curve offered to RC by an output port multiplexer)**.** *Consider the output port defined in Fig.1 with a constant rate C, and serving the traffic classes $k \in \{SCT, RC, BE\}$. Consider α_k-constrained traffic class k, the strict minimum service curve offered to the RC class by the output port multiplexer is:*

$$\beta^{mux}_{RC}(t) = \max\left(\beta^{sp}_{RC}, \beta^{bls}_{RC}\right)(t)$$

with:

- $\beta^{sp}_{RC}(t) = (C\cdot t - \alpha_{SCT} \oslash \beta^{bls}_{SCT}(t) - \max_{f\in All} MFS_f)_\uparrow$;
- $\beta^{bls}_{RC}(t) = (C \cdot t - \gamma^{bls}_{SCT}(t) - \max_{f\in All} MFS_f)_\uparrow$;
- $\gamma^{bls}_{SCT}(t)$ *and* β^{bls}_{SCT} *the maximum and strict minimum service curves offered by the BLS node to SCT defined in Th.4 and Th.3, respectively, and $All = \{SCT \cup RC \cup BE\}$.*

Proof. The proof of Th.6 is straightforward. Th.6 is obtained through replacing the arrival curve of higher priority traffic than RC, i.e., SCT, by the curve computed in Cor.2 within the equation of Corollary 1. □

IV. Performance Evaluation

In this section, we conduct performance analysis of the proposed extended AFDX (implementing the BLS) to evaluate its efficiency to support mixed-criticality data, in comparison to the current AFDX solution, i.e., AFDX with regular 3-priority NP-SP scheduler. This evaluation is based on the worst-case timing analysis detailed in Section III. First, we describe our case study. Afterwards, we assess the tightness of our proposed model for the extended AFDX, in reference to the simulation results obtained in [4]. Finally, we analyse the impact of our proposal on SCT and RC performance when varying traffic utilisation rates, in comparison to the current AFDX.

A. Case Study

We consider a Gigabit extended AFDX switch described in Fig.3, and with the input traffic described in Table II. The switch is connected to 4 Gigabit cables for each type of input traffic and one Gigabit cable for the output traffic. The number of SCT flows enqueued in an output port, denoted n^{in}_k, determines the load of the output port. We denote UR_k the utilisation rate of class $k \in \{SCT, RC\}$, which directly depends on n^{in}_k: $UR_k = n^{in}_k \cdot \frac{MFS_k}{BAG_k}$.

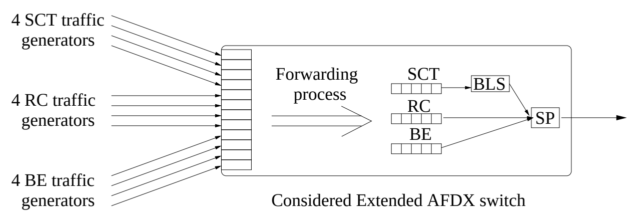

Fig. 3. Output port multiplexer node nomenclature

Priority	Traffic type	MFS (Bytes)	BAG (ms)
0/2	SCT	64	2
1	RC	320	2
3	BE	1024	8

TABLE II
Avionics flow Characteristics

Scenarios	Scenario 1	Scenario 2
$(UR_{SCT}; UR_{RC})(\%)$	$([0.1:0.1:78]; 20)$	$(20; [0.5:0.5:72])$
$(BW; L_M; L_R)$ $(\%; bits; bits)$	$(46; 22118; 0)$	$(46; 22118; 0)$

TABLE III
Parameters considered for testing scenarios 1 and 2

Moreover, we consider 2 scenarios described in Table III. The aim of scenario 1 (resp. 2) is to get an idea on the impact of increasing the SCT (resp. RC) utilisation rate on RC and SCT delay bounds. In particular, we want to verify if the deadlines are fulfilled for both SCT and RC when varying the load of the network.

Thus, in scenario 1 (resp. 2), we set RC (resp. SCT) flows input rates at 20%, which means generating 156 (resp. 790) flows. Then, we vary SCT (resp. RC) utilisation rate, UR_{SCT} (resp. UR_{RC}) from 0 to over 70%. BE is used to bring the load up to 100% and we do not present its timing results, since it does not have a deadline. The BLS parameters are the same in both scenarios as detailed in Table III: L_R is set to its minimum value, L_M is set to absorb a burst of 80 SCT frames and BW is just below its median (0.5) value.

In addition to the delay bounds computed with our analytical model, we present the simulation results from [4] obtained with ns-2 simulations to assess the model tightness. Each conducted simulation has a duration of 5s, which represents up to 3.2 millions SCT and RC simulated frames. The results of scenarios 1 and 2 are presented in Figures 4 and 5, respectively.

B. Tightness analysis

As illustrated in Figures 4 and 5, simulation results and the analytical delay bounds computed for the extended AFDX (BLS on top of NP-SP) are very similar and the corresponding curves have the same shape. Moreover, the maximum gap between both curves for SCT (resp. RC) is varying between 0.1% (resp. 0.1%) and 24% (resp. 29%). This gap is increasing with the utilization rate, since it becomes more and more difficult to catch the worst-case scenario with simulation under an increasing number of transmitted messages.

These results show the good tightness of our proposed model based on Network Calculus.

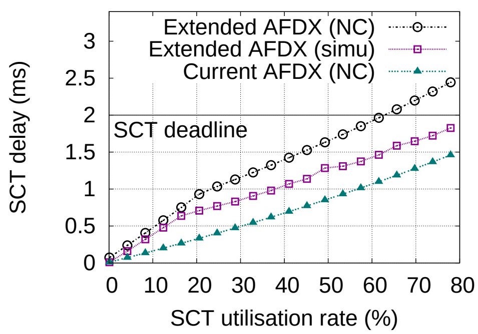

(a)

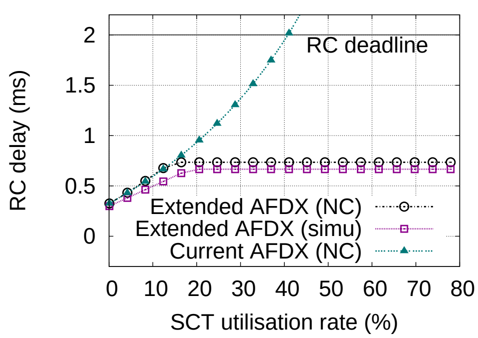

(b)

Fig. 4. Scenario 1: Impact of SCT max. utilisation rate on: (a) SCT delays; (b) RC delays

C. Analytical delay bound analysis

The results of varying SCT utilisation rate are presented in Fig.4. We can see that the SCT delay bound is increased by the extended AFDX (see Fig.4(a)), comparatively to current AFDX. This is due to the BLS behaviour: our extended AFDX consists of a BLS node and a NP-SP node, and depending on the BLS parameters and the traffic flows, one is predominant on the other. This is confirmed by the RC delay bounds (see Fig.4(b)). For instance, below 12% of SCT utilisation rate, the current and extended AFDX curves of the RC delay bounds are overlapping; thus the NP-SP part is predominant. After 12% they diverge, showing that BLS has now a stronger impact. While the delay bound of RC with current AFDX soars, it remains constant with our extended AFDX thanks to the BLS node. This shows the good isolation level provided to RC traffic by the BLS. In fact, while the BLS increases the SCT delay bound by 1.0ms, it decreases the RC delay bound by 7.3ms. As a result, the RC delay bound is much reduced with our extended AFDX, while the SCT delay bound is only slightly increased. It is also worth noting that with the current AFDX the RC deadline is reached at a SCT utilisation rate of 40%, while it is reached at 60% with the extended AFDX. This represents a gain of 50% in terms of SCT utilisation rate.

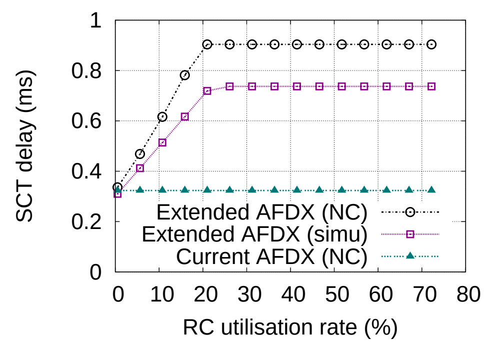

(a)

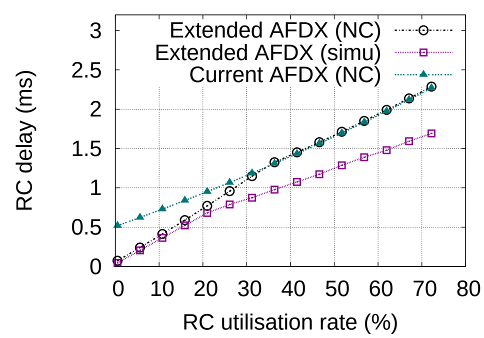

(b)

Fig. 5. Scenario 2: Impact of RC max. utilisation rate on: (a) SCT delays; (b) RC delays

The results of varying RC utilisation rate are presented in Fig.5. As before, we can see that the SCT delay bound is increased under the extended AFDX (see Fig.5(a)), but remains well below its deadline at 2ms. On the other hand, the RC delay bound is either improved with the extended AFDX or remains the same as the current AFDX. Additionally, we can see that with the chosen BLS parameters, the BLS has a stronger impact under low RC utilisation rate. For instance, in Fig.5(b), there is a gap between the RC analytical delay bounds computed under both extended and current AFDX solutions, which decreases as RC utilisation rate increases. Indeed, when the RC utilisation rate increases, the impact of the BLS on RC traffic decreases until it becomes negligible. Then, only NP-SP rules the RC delay bound behaviour. This shows that the RC delay bound can be improved by the BLS (up to 77%). At the current utilisation rate of the AFDX (30% on the 100 Mbps AFDX network, so 3% on a Gigabit AFDX), the gain in terms of delay bound for RC traffic is around 60% with the extended AFDX, compared to current AFDX. This gain is still over 25% for an RC utilisation rate at 15%.

These results show the ability of extended AFDX (incorporating the BLS) to favour the predictability and fairness properties since it enables a noticeable RC delay bound decrease, while guaranteeing the SCT and RC deadlines.

V. CONCLUSIONS

In this paper, we have proposed a model and a timing analysis using Network Calculus of an extended AFDX network, to handle mixed-criticality avionics applications. The extended AFDX implements a BLS shaper on top of NP-SP scheduler within AFDX switches to manage three priority levels. The conducted performance evaluation highlights the tightness of the proposed model, in reference to simulation results. Moreover its confirms the benefit of using the BLS to isolate the highest priority (SCT), and mitigate its impact on the medium one (RC). For instance, numerical results have shown noticeable enhancements of the delay upper bounds of the RC traffic (up to 77%) and a gain in terms of maximum utilisation rate up to 50% for SCT under the extended AFDX, in comparison with the current one.

Our results may be generalized to the case of multi-hop networks. Moreover, we plan their generalization to the case where more than one class is submitted to a BLS shaper.

APPENDIX

In this appendix, we present the proofs of the strict minimum and maximum service curves defined in Th.3 and Th.4, respectively. First, we present three lemmas common to the two proofs, then we continue with the theorem proofs.

A. Continuous-credit Lemmas

We consider $R^*_{SCT}(t)$ the output cumulative traffic function of class SCT and $\Delta R^*_{SCT}(\delta)$ its variation during δ.

The BLS credit tries to keep an accurate accounting of the traffic sent. There are two situations when it loses track due to non-preemptive transmissions:

1) when the credit reaches L_M and the current SCT frame has not finished its transmission;
2) when the credit reaches 0 and the current RC frame has not finished its transmission.

The credit saturation at L_M can only occur when a SCT frame is being transmitted, while the saturation at 0 can occur when a RC frame is being transmitted. We call this the saturation of the credit, either at L_M by SCT traffic or at 0 by RC traffic.

Hence, we call $\Delta R^*_{L_M,sat}(\delta)$ (resp.$\Delta R^*_{0,sat}(\delta)$) the part of $\Delta R^*_{SCT}(\delta)$ (resp. $\delta \cdot C - \Delta R^*_{SCT}(\delta)$), that can be sent during any interval δ while the credit is saturated at L_M (resp. at 0).

We present here three lemmas linked to the credit saturation and necessary to both theorem proofs. First in Lemma 1, we show how to bound the sum of the consumed and gained credits, depending on the credit saturations. Then, we detail the bounds of traffic sent during the credit saturations at 0 and L_M in Lemma 2 and Lemma 3, respectively.

Lemma 1 (Continuous-credit bounds)**.** *We consider the shaped class SCT with a maximum credit level L_M. $\forall\delta$, the sum of the consumed and gained credits is characterized by:*

$$L_M \geqslant \begin{pmatrix} \Delta R^*_{SCT}(\delta) - \dfrac{\Delta R^*_{L_M,sat}(\delta)}{C} \cdot I_{send} \\ -(\delta - \dfrac{\Delta R^*_{0,sat}(\delta)}{C}) \cdot I_{idle} \end{pmatrix} \geqslant -L_M$$

Proof. In an interval δ, the accurate consumed credit is the product of time it takes to send the SCT traffic when the credit is not saturated at L_M $\frac{\Delta R^*_{SCT}(\delta) - \Delta R^*_{L_M,sat}(\delta)}{C}$ and the sending slope I_{send}:

$$credit_{consumed} = \left(\frac{\Delta R^*_{SCT}(\delta) - \Delta R^*_{L_M,sat}(\delta)}{C}\right) \cdot I_{send}$$

Conversely, the accurate gained credit is the product of the remaining time of δ (when the credit is not saturated at 0 and the SCT traffic is not sent) and the signed idle slope $-I_{idle}$:

$$credit_{gained} = \left(\delta - \frac{\Delta R^*_{SCT}(\delta) + \Delta R^*_{0,sat}(\delta)}{C}\right) \cdot (-I_{idle})$$

Therefore, knowing that $I_{send} + I_{idle} = C$, the sum of the gained and the consumed credits $\forall\delta \in \mathbb{R}^+$ is:

$$\begin{aligned} & credit_{consumed} + credit_{gained} \\ &= (\frac{\Delta R^*_{SCT}(\delta) - \Delta R^*_{L_M,sat}(\delta)}{C}) \cdot (I_{send}) \\ &+(\delta - \frac{\Delta R^*_{SCT}(\delta) + \Delta R^*_{0,sat}(\delta)}{C}) \cdot (-I_{idle}) \\ &= \Delta R^*_{SCT}(\delta) - \frac{\Delta R^*_{L_M,sat}(\delta)}{C} \cdot I_{send} \\ &-(\delta - \frac{\Delta R^*_{0,sat}(\delta)}{C}) \cdot I_{idle} \end{aligned}$$

Knowing that the credit is a continuous function with a lower bound 0 and an upper bound L_M, we have:

$$L_M \geqslant \quad credit_{consumed} + credit_{gained} \quad \geqslant -L_M$$

$$L_M \geqslant \begin{pmatrix} \Delta R^*_{SCT}(\delta) - \dfrac{\Delta R^*_{L_M,sat}(\delta)}{C} \cdot I_{send} \\ -(\delta - \dfrac{\Delta R^*_{0,sat}(\delta)}{C}) \cdot I_{idle} \end{pmatrix} \geqslant -L_M$$

□

Lemma 2 (Credit saturation at 0)**.** *We consider a shaped class SCT. $\forall\delta$, the amount of traffic sent while the credit is saturated at 0, denoted $\Delta R^*_{0,sat}(\delta)$, is bounded by:*

$$0 \leqslant \Delta R^*_{0,sat}(\delta) \leqslant MFS^{sat}_{RC} \cdot \left(\frac{\delta}{\Delta^{\beta}_{inter}} + 1\right)$$

with:

$$MFS^{sat}_{RC} = \max\left(\max_{f\in RC} MFS_f - \frac{C}{I_{idle}} \cdot L_R, 0\right)$$
$$\Delta^{\beta}_{inter} = \frac{\max_{f\in RC} MFS_f}{C} + \frac{L_M - L^{min}_R}{I_{send}} + \frac{L_M - L_R}{I_{idle}}$$
$$L^{min}_R = \max(L_R - \frac{\max_{f\in RC} MFS_f}{C} \cdot I_{idle}, 0)$$

Proof. First, we know that $\Delta R^*_{0,sat}(\delta) \geqslant 0$. Secondly, we consider only the impact of RC on SCT within the BLS node bls, since the impact of BE is taken into account in the NP-SP node sp.

In the presence of SCT frames, the saturation of the credit at 0 can occur if an additional RC frame is sent, while the credit is decreasing and about to reach L_R. Due to non-preemption, the frame finishes its transmission even though the SCT priority is now higher.

To compute the largest impact of the non-preempted RC frames on SCT traffic, we need the highest number of non-preempted RC frames that can be sent during a time interval δ; thus the smallest duration between two occurrences of such a situation. Fig.6 illustrates such a duration.

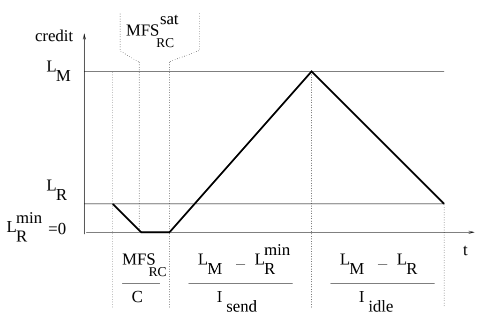

Fig. 6. Computing $\beta^{bls}_{SCT}(t)$

In presence of SCT traffic, no RC traffic can be sent until a priority change: L_M must be reached between two non-preempted RC frames.

Thus, we study the intervals of time between two starts of transmission of non-preempted RC frame just before the credit reaches L_R. The smallest duration of such an interval, Δ^{β}_{inter}, is equal to the sum of

1) the transmission time of the non-preempted RC frame, such as at the end of the transmission the credit reaches $L^{min}_R = \max(L_R - \frac{\max_{f\in RC} MFS_f}{C} \cdot I_{idle}, 0)$;
2) the duration $\frac{L_M - L^{min}_R}{I_{send}}$ because SCT traffic has to be sent continuously in order for the credit to reach L_M in the minimum duration;
3) the duration $\frac{L_M - L_R}{I_{idle}}$ because RC traffic has to be sent continuously in order for the credit to return in the minimum duration to L_R.

Consequently,

$$\Delta^{\beta}_{inter} = \frac{\max_{f\in RC} MFS_f}{C} + \frac{L_M - L^{min}_R}{I_{send}} + \frac{L_M - L_R}{I_{idle}}$$

Thus during δ, the number of non-preempted RC frames (sent when the credit reaches L_R) is upper bounded by $\lceil \frac{\delta}{\Delta^{\beta}_{inter}} \rceil$.

Finally, we need to compute the maximum traffic sent while the credit remains at 0, as illustrated in Fig.6. This is equal to the maximum size of a RC frame, minus the amount of data transmitted while the credit decreases from L_R to 0:

$$MFS^{sat}_{RC} = \max(\max_{f\in RC} MFS_f - \frac{C}{I_{idle}} \cdot L_R, 0).$$

As a result, the RC traffic sent while the credit is saturated at 0 is as follows:

$$\Delta R^*_{0,sat}(\delta) \leqslant MFS^{sat}_{RC} \cdot \lceil \frac{\delta}{\Delta^{\beta}_{inter}} \rceil$$
$$\leqslant MFS^{sat}_{RC} \cdot \left(\frac{\delta}{\Delta^{\beta}_{inter}} + 1\right)$$

□

Lemma 3 (Credit saturation at L_M)**.** *We consider a shaped class SCT. $\forall\delta$, the amount of traffic sent while the credit is saturated at L_M, denoted $\Delta R^*_{L_M,sat}(\delta)$, is bounded by:*

$$0 \leqslant \Delta R^*_{L_M,sat}(\delta) \leqslant \max_{f\in SCT} MFS_f \cdot \left(\frac{\delta}{\Delta^{\gamma}_{inter}} + 1\right)$$

with:

$$\Delta^{\gamma}_{inter} = \frac{\max_{f\in SCT} MFS_f}{C} + \frac{L_M - L_R}{I_{idle}} + \frac{L_M - L_R}{I_{send}}$$

Proof. First, we know that $\Delta R^*_{L_M,sat}(\delta) \geqslant 0$. Secondly, the saturation of the credit at L_M can only occur if an SCT frame is sent while the credit is increasing and about to reach L_M. Due to non-preemption, the SCT frame finishes its transmission even though the SCT priority is now lower.

To be able to compute the largest impact of the non-preempted SCT frames, we need the highest number of non-preempted SCT frames that can be sent during a time interval δ; thus the smallest duration between two occurrences of such a situation. Fig.7 illustrates such a duration. In presence of RC traffic, no SCT traffic can be sent until a priority change: L_R must be reached between two non-preempted SCT frames.

Thus, we study the intervals of time between two starts of transmission of non-preempted SCT frame just before L_M is reached. The smallest duration of such an interval, Δ^{γ}_{inter}, is equal to the sum of:

1) the transmission time of the non-preempted SCT frame (at the end of the transmission the credit is equal to L_M);

2) the duration $\frac{L_M - L_R}{I_{idle}}$ because RC traffic has to be sent continuously in order for the credit to reach L_R in the minimum duration;
3) the duration $\frac{L_M - L_R}{I_{send}}$ because SCT traffic has to be sent continuously in order for the credit to return in the minimum duration to L_M.

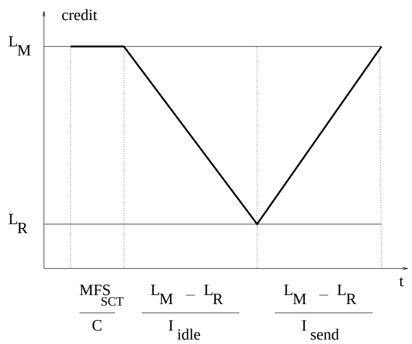

Fig. 7. Computing $\gamma^{bls}_{SCT}(t)$

Consequently,

$$\Delta^{\gamma}_{inter} = \frac{\max_{f\in SCT} MFS_f}{C} + \frac{L_M - L_R}{I_{idle}} + \frac{L_M - L_R}{I_{send}}$$

Thus during δ, the number of non-preempted SCT frames (sent when the credit reaches L_M) is upper bounded by $\lceil \frac{\delta}{\Delta^{\gamma}_{inter}} \rceil$.

As a result, the SCT traffic sent while the credit is saturated at L_M is as follows:

$$\begin{aligned}\Delta R^*_{L_M,sat}(\delta) \quad &\leqslant \quad \max_{f\in SCT} MFS_f \cdot \lceil \frac{\delta}{\Delta^{\gamma}_{inter}} \rceil \\ &\leqslant \quad \max_{f\in SCT} MFS_f \cdot \left(\frac{\delta}{\Delta^{\gamma}_{inter}} + 1 \right)\end{aligned}$$

□

B. Proof of Theorem 3

We search a strict minimum service curve offered to SCT defined by a rate-latency curve, i.e., $\beta^{bls}_{SCT}(t) = \rho \cdot (t-\tau)^+$ with rate ρ and initial latency τ.

According to the definition of the strict minimum service curve, $\forall$ backlogged period δ:

$$\Delta R^*_{SCT}(\delta) \geqslant \beta^{bls}_{SCT}(\delta) = \rho \cdot (\delta - \tau)^+ \tag{2}$$

For any duration lower than τ, the variation of the SCT output cumulative traffic is lower bounded by 0.

$$\forall \delta \leqslant \tau, \Delta R^*_{SCT}(\delta) \geqslant 0$$

Thus, the best τ for the strict minimum service curve is the largest duration during which no SCT traffic can be sent. So, when considering only the impact of RC class, the worst-case duration τ occurs if the credit starts at L_M: RC frames are transmitted until L_R is reached and an additional RC frame is sent due to non-preemption. We denote this duration Δ^{β}_{idle}:

$$\Delta^{\beta}_{idle} = \frac{L_M - L_R}{I_{idle}} + \frac{\max_{f\in RC} MFS_f}{C}$$

Hence, we have the service latency: $\tau = \Delta^{\beta}_{idle}$

Concerning the ρ, we use the definition of β^{bls}_{SCT} as a rate-latency curve and Eq.(2) to deduce a property of ρ:

$$\lim_{\delta\to+\infty} \frac{\Delta R^*_{SCT}(\delta)}{\delta} \geqslant \lim_{\delta\to+\infty} \rho \cdot \left(1 - \frac{\tau}{\delta}\right) = \rho.$$

We now use the continuity property of the BLS credit to determine ρ. From Lemma 1, we know that:

$$\begin{pmatrix} \Delta R^*_{SCT}(\delta) - \dfrac{\Delta R^*_{L_M,sat}(\delta)}{C} \cdot I_{send} \\ -(\delta - \dfrac{\Delta R^*_{0,sat}(\delta)}{C}) \cdot I_{idle} \end{pmatrix} \geqslant -L_M$$

$$\begin{aligned}\Rightarrow \Delta R^*_{SCT}(\delta) \quad &\geqslant \quad -L_M + \frac{\Delta R^*_{L_M,sat}(\delta)}{C} \cdot I_{send} \\ &\quad\quad +(\delta - \frac{\Delta R^*_{0,sat}(\delta)}{C}) \cdot I_{idle}\end{aligned}$$

$$\begin{aligned}\Rightarrow \frac{\Delta R^*_{SCT}(\delta)}{\delta} \quad &\geqslant \quad \frac{-L_M}{\delta} + \frac{\Delta R^*_{L_M,sat}(\delta)}{\delta \cdot C} \cdot I_{send} \\ &\quad\quad +(1 - \frac{\Delta R^*_{0,sat}(\delta)}{\delta \cdot C}) \cdot I_{idle}\end{aligned}$$

$$\begin{aligned}\lim_{\delta\to+\infty} \frac{\Delta R^*_{SCT}(\delta)}{\delta} \geqslant \quad \lim_{\delta\to+\infty} \quad &\frac{-L_M}{\delta} + \frac{\Delta R^*_{L_M,sat}(\delta)}{\delta \cdot C} \cdot I_{send} \\ &+(1 - \frac{\Delta R^*_{0,sat}(\delta)}{\delta \cdot C}) \cdot I_{idle}\end{aligned} \tag{3}$$

Using Lemmas 2 and 3, the lower bound of $\Delta R^*_{L_M,sat}(\delta)$ and the upper bound of $\Delta R^*_{0,sat}(\delta)$ are as follows:

$$\lim_{\delta\to\infty} \frac{\Delta R^{*,max}_{L_M,sat}(\delta)}{\delta} \geqslant 0 \tag{4}$$

$$\lim_{\delta\to\infty} \frac{\Delta R^{*,max}_{0,sat}(\delta)}{\delta} \leqslant \frac{MFS^{sat}_{RC}}{\Delta^{\beta}_{inter}} \tag{5}$$

Thus, from Eq.(3), Eq.(4), and Eq.(5), we deduce:

$$\begin{aligned}\lim_{\delta\to+\infty} \frac{\Delta R^*_{SCT}(\delta)}{\delta} \quad &\geqslant \quad \lim_{\delta\to+\infty} (1 - \frac{\Delta R^{*,max}_{0,sat}(\delta)}{\delta \cdot C}) \cdot I_{idle} \\ &= \quad \left(C - \frac{MFS^{sat}_{RC}}{\Delta^{\beta}_{inter}} \right) \cdot \frac{I_{idle}}{C}\end{aligned}$$

Finally, a suitable ρ is as follows:

$$\rho = \left(C - \frac{MFS^{sat}_{RC}}{\Delta^{\beta}_{inter}} \right) \cdot \frac{I_{idle}}{C}.$$

C. Proof of Theorem 4

We search a maximum service curve offered to SCT defined by a leaky-bucket curve, i.e., $\gamma^{bls}_{SCT}(t) = r \cdot t + b$ with rate r and burst b.

According to the definition of the maximum service curve, for any δ beginning at the start of the backlogged period of SCT:

$$\forall \delta, \Delta R^*_{SCT}(\delta) \leqslant \gamma^{bls}_{SCT}(\delta) = r \cdot \delta + b \tag{6}$$

In the absence of other traffic, SCT can use the full capacity of the link; thus $\Delta R^*_{SCT}(\delta) \leqslant C \cdot t$ and $\gamma^{bls}_{SCT}(t) = C \cdot t$. In a RC backlogged period, we use the definition of γ^{bls}_{SCT} as a leaky-bucket maximum service curve to deduce the following property of r using Eq. (6):

$$\lim_{\delta \to +\infty} \frac{\Delta R^*_{SCT}}{\delta} \leqslant \lim_{\delta \to +\infty} r + \frac{b}{\delta} = r.$$

We use the continuity property of the BLS credit to determine r. From Lemma 1, we know that:

$$\Delta R^*_{SCT}(\delta) - \frac{\Delta R^*_{L_M,sat}(\delta)}{C} \cdot I_{send} - (\delta - \frac{\Delta R^*_{0,sat}(\delta)}{C}) \cdot I_{idle} \leqslant L_M$$

$$\Rightarrow \Delta R^*_{SCT}(\delta) \leqslant L_M + \frac{\Delta R^*_{L_M,sat}(\delta)}{C} \cdot I_{send} + (\delta - \frac{\Delta R^*_{0,sat}(\delta)}{C}) \cdot I_{idle}$$

$$\Rightarrow \frac{\Delta R^*_{SCT}(\delta)}{\delta} \leqslant \frac{L_M}{\delta} + \frac{\Delta R^*_{L_M,sat}(\delta)}{\delta \cdot C} \cdot I_{send} + (1 - \frac{\Delta R^*_{0,sat}(\delta)}{\delta \cdot C}) \cdot I_{idle}$$

$$\lim_{\delta \to +\infty} \frac{\Delta R^*_{SCT}(\delta)}{\delta} \leqslant \lim_{\delta \to +\infty} \frac{L_M}{\delta} + \frac{\Delta R^*_{L_M,sat}(\delta)}{\delta \cdot C} \cdot I_{send} + (1 - \frac{\Delta R^*_{0,sat}(\delta)}{\delta \cdot C}) \cdot I_{idle} \tag{7}$$

Using Lemmas 2 and 3, the upper bound of $\Delta R^*_{L_M,sat}(\delta)$ and the lower bound of $\Delta R^*_{0,sat}(\delta)$ are as follows:

$$\lim_{\delta \to \infty} \frac{\Delta R^{*,max}_{0,sat}(\delta)}{\delta} \geqslant 0$$

$$\lim_{\delta \to \infty} \frac{\Delta R^{*,max}_{L_M,sat}(\delta)}{\delta} \leqslant \frac{\max_{f \in SCT} MFS_f}{\Delta^{\gamma}_{inter}}.$$

Thus, from Eq. (7), we deduce:

$$\begin{aligned} \lim_{\delta \to +\infty} \frac{\Delta R^*_{SCT}(\delta)}{\delta} &\leqslant \lim_{\delta \to +\infty} I_{idle} + \frac{\Delta R^{*,max}_{L_M,sat}(\delta)}{\delta \cdot C} \cdot I_{send} \\ &= I_{idle} + \frac{\max_{f \in SCT} MFS_f}{\Delta^{\gamma}_{inter}} \cdot \frac{I_{send}}{C} \\ &= \frac{\Delta^{\gamma}_{send}}{\Delta^{\gamma}_{inter}} \cdot C < C \end{aligned} \tag{8}$$

where:

$$\Delta^{\gamma}_{send} = \frac{\max_{f \in SCT} MFS_f}{C} + \frac{L_M - L_R}{I_{send}}$$

Finally, a suitable rate r is : $r = \frac{\Delta^{\gamma}_{send}}{\Delta^{\gamma}_{inter}} \cdot C$

Now that we have found r, we need to find b such as:

$$\Delta R^*_{SCT}(\delta) \leqslant \frac{\Delta^{\gamma}_{send}}{\Delta^{\gamma}_{inter}} \cdot C \cdot \delta + b$$

In the presence of RC traffic, the largest period of time during which SCT traffic can be sent continuously occurs if the credit started at 0. Then, SCT traffic is sent continuously until L_M is reached and the priority is changed to its low value p_L. If a new SCT frame starts its transmission just before the credit reached L_M due to non-preemption, it will finish its transmission before the waiting RC traffic can be sent. Thus, with a link capacity C the largest SCT burst is $b^{max}_{SCT} = \frac{C}{I_{send}} \cdot L_M + \max_{f \in SCT} MFS_f$, and consequently:

$$\Delta R^*_{SCT}(\frac{b^{max}_{SCT}}{C}) \leqslant b^{max}_{SCT} = \frac{\Delta^{\gamma}_{send}}{\Delta^{\gamma}_{inter}} \cdot b^{max}_{SCT} + b$$

$$\Rightarrow b = b^{max}_{SCT} \cdot \frac{\Delta^{\gamma}_{idle}}{\Delta^{\gamma}_{inter}}$$

with $\Delta^{\gamma}_{idle} = \frac{L_M - L_R}{I_{idle}}$. So, we have proved that $\forall \delta \in \mathbb{R}^+$:

$$\Delta R^*_{SCT}(\delta) \leqslant \frac{\Delta^{\gamma}_{send}}{\Delta^{\gamma}_{inter}} \cdot C \cdot \delta + b^{max}_{SCT} \cdot \frac{\Delta^{\gamma}_{idle}}{\Delta^{\gamma}_{inter}}.$$

References

[1] Airlines Electronic Engineering Committee. Aircraft Data Network Part 7, Avionics Full Duplex Switched Ethernet (AFDX) Network, ARINC Specification 664. Aeronautical Radio, 2002.

[2] Anne Bouillard, Laurent Jouhet, and Eric Thierry. Service curves in Network Calculus: dos and don'ts. Research report, INRIA, 2009.

[3] Markus Fidler, Volker Sander, and Wojciech Klimala. Traffic shaping in aggregate-based networks: implementation and analysis. *Computer Communications*, 2005.

[4] Anaïs Finzi, Ahlem Mifdaoui, Emmanuel Lochin, and Fabrice Frances. Incorporating TNS/BLS in the AFDX for Mixed-Criticality Avionics Applications: Specification. In *ERTS2*, 2018.

[5] Christian M Fuchs et al. The evolution of avionics networks from ARINC 429 to AFDX. *Network Architectures and Services*, 2012.

[6] Franz-Josef Gotz. Traffic Shaper for Control Data Traffic (CDT). *IEEE 802 AVB Meeting*.

[7] Jérôme Grieu. *Analyse et évaluation de techniques de commutation Ethernet pour l'interconnexion des systèmes avioniques*. PhD thesis, INPT, 2004.

[8] J.Y. Le Boudec and P. Thiran. *Network calculus: a theory of deterministic queuing systems for the internet*. Springer-Verlag, 2001.

[9] Jork Loeser and Hermann Haertig. Low-latency hard real-time communication over switched ethernet. In *ECRTS*, 2004.

[10] Zhao Luxi, Pop Paul, Li Qiao, Chen Junyan, and Xiong Huagang. Timing analysis of rate-constrained traffic in TTEthernet using network calculus. *Real-Time Systems*, 2017.

[11] R. Bosch GmbH. CAN specification Version 2,0. Technical report, 1991.

[12] F.-J. Gotz S. Kerschbaum and F. Chen. Towards the Calculation of Performance Guarantees for BLS in Time-Sensitive Networks. *IEEE 802.1 TSN Meeting*, 2013.

[13] N. Concer S. Thangamuthu, P. Cuijpers JL, and J. Lukkien. Analysis of ethernet-switch traffic shapers for in-vehicle networking applications. In *DATE*, 2015.

[14] Perathoner Simon, Wandeler Ernesto, Thiele Lothar, and et al. Influence of different abstractions on the performance analysis of distributed hard real-time systems. *Design Automation for Embedded Systems*, 2009.

[15] D. Thiele and R. Ernst. Formal worst-case timing analysis of Ethernet TSN's burst-limiting shaper. In *DATE*, 2016.